# Order-$n$ Formulation of Extrusion of a Beam with Large Bending and Rotation

Arun K. Banerjee*
*Lockheed Missiles & Space Company, Sunnyvale, California 94089*

**Rosenthal's order-$n$ algorithm for formulating equations of motion of an $n$-degree-of-freedom multibody system is adapted to a situation where $n$ itself changes with time according to a prescribed motion. Effectiveness of modeling a beam in this context by a series of rigid rods connected by rotational springs is demonstrated by comparison to a conventional approach using time-varying shape functions. The formulation is capable of describing large bending deformation of a beam undergoing large overall motion. This is illustrated by three simulations: extrusion/retraction of a beam from/into a base undergoing planar rotation, retraction of a tether into a rotating base, and three-dimensional deformation of a long antenna during spin-up of its base undergoing nonplanar rotation.**

## Introduction

ANY standard formulation of the equations of motion of a multiple-rigid-body system gives rise to a high-order, dense mass matrix. It can be shown that the procedure used to form the coefficients of the mass matrix and then to uncouple the equations with respect to the highest time derivative of the dependent variables requires $\mathcal{O}(n^3)$ arithmetic operations, where $n$ is the number of degrees of freedom of the system. Formulation of equations of motion in a manner that results in $\mathcal{O}(n)$ operation counts for performing the same task recently has been a subject of intense research in the field of multibody dynamics (see, e.g., Refs. 1–6) for the obvious reason that an $\mathcal{O}(n)$ algorithm requires far fewer computations than an $\mathcal{O}(n^3)$ formulation when $n$ is large. There is a basic similarity in the $\mathcal{O}(n)$ formulations published so far in that all use recursive methods in three passes: a forward pass to construct the kinematics, a backward pass to get the first dynamical equation, and a final forward pass to get the rest of the dynamical equations. The method behind order-$n$ formulations is not unique. For example, Hollerbach[1] uses Lagrange's equations, Rosenthal[2] uses Kane's equations, Rodriguez[3] uses the filtering and smoothing approach of optimal estimation in deriving the equations, Bae and Haug[4] use the method of virtual work, Roberson and Schwertassek[5] use the Newton-Euler method, and Keat[6] uses a velocity transformation approach.

A class of problems to which the order-$n$ formulation has not been applied so far is described by a situation where the degree-of-freedom $n$ itself changes with time. This happens, for example, when a beam represented by a finite number of segments is extruded or retracted from or into a second rotating body. The Shuttle-based U.S./Canada waves in space plasma (WISP) experiment, in which two antennae will be extended from 0 to 150 m, held at that length, and then retracted into the Shuttle while the latter rotates slowly in yaw or roll, provides an application of this type of a dynamical system. References 7–11 are, in essence, devoted to this problem where the authors were concerned with describing the bending vibration of a cantilever beam whose length changed with time. These references used small deflection beam theory and assumed deformations in the form of modes or admissible functions whose spatial argument contained the time-varying length of the beam.

The basic constraint involved in relative translation of a flexible body with respect to another body has been studied by Li and Likins[12] in terms of a translation coordinate and modes dependent on it, whereas Hwang and Haug[13] showed the influence of global modes and substructuring on the response in this context. The convention of using time-varying modes to describe deployment dynamics might appear as intuitively appealing, but it is only an assumption, the validity of which has not been rigorously proved. This consideration had led the authors of Ref. 14 to use a model of the beam where the beam was discretized into a number of rigid links connected by rotational springs, and extrusion/retraction was described by increasing/decreasing the number of links; to reduce the order of this model, use was made in Ref. 14 of the small deformation vibration modes for the number of links that were deployed at any given time. Although both Refs. 11 and 14, dealing directly with the WISP problem, were restricted to small deflection beam theory, indications were presented in Ref. 11 of the distinct possibility of occurrence of large bending during extrusion/retraction. This paper is about a simulation tool to describe such large bending deformations. Because the superposition used in any modal approach is untenable for nonlinear elastic deformation, whereas the discretized beam representataion of Ref. 14 can describe large bending, the latter is the model preferred in this paper.

The contribution of this paper is as follows. Rosenthal's order-$n$ algorithm is adapted to handle situations with variable $n$ and prescribed base motion. Next, with a view to applying this formulation to a segmented rigid/elastic system undergoing deployment, the effectiveness of such a model is established by comparison to a modal-type model for deployment of a beam with small elastic deflections. The variable $n$ order-$n$ algorithm is then used to generate new results on large bending of a beam during extrusion/retraction from/into a rotating base. It is shown how the present analysis can reproduce a well-known result of retrieval of a tether, which is a beam with no bending stiffness, into an orbiting satellite. Finally, a simulation of large bending during spin-up of a long, slender boom attached to a base undergoing nonplanar rotation is given to illustrate use of the algorithm to describe three-dimensional motion. The capability of efficiently simulating large bending of a beam, during extension/retraction or at fixed length, as demonstrated in this paper, will be of crucial importance in the selection of deployment or spin-up rates, and eventually control, of the WISP antenna.

Presented as Paper 90-1235 at the AIAA Dynamics Specialist Conference, Long Beach, CA, April 5–6, 1990; received June 15, 1990; revision received Jan. 9, 1991; accepted for publication Jan. 10, 1991.


*Senior Staff Engineer, Org. 92-30, Bldg. 281.

## Model Description

The beam being extruded from a rotating base is modeled as a system of rigid links connected by rotational springs, as in Ref. 14; a schematic representation of this is given in Fig. 1. At any given time $t$, the system consists of a rigid body $B$ whose motion is prescribed a priori in a Newtonian frame $N$, and rigid massless links $E_i$ $(i = 1, \ldots, n)$ each of length $L$ connected to each other by revolute joints with particles of masses $m_i$ $(i = 1, \ldots, n)$ located at the ends of the links; linear torsion springs of stiffness $k_i$ resist the rotation between two adjacent links for all of the revolute joints. For an equivalent representation of the actual elastic beam of linear mass density $\rho$ and flexural rigidity $EI$ by this model, the masses $m_i$ and the stiffness $k_i$ have the values

$$m_i = \rho L \qquad (i = 1, \ldots, n) \tag{1}$$

$$k_1 = \frac{EI}{L} \tag{2a}$$

$$k_2 = \frac{6(n-1)EI}{(3n-1)L} \tag{2b}$$

$$k_i = k_1 \qquad (i = 1, \ldots, n-1) \tag{2c}$$

$$k_n = k_2 + (k_1 - k_2)d/L \tag{2d}$$

where $d$ is the distance from a point O fixed in B to the anchor point A for the beam. Here, the stiffness coefficients are obtained by equating the deflections of a Bernoulli-Euler beam due to a tip load to the deflections of the discretized beam at all points where the rotational springs are attached. An extrusion/retraction process is modeled by treating the number of links $n$ as a discontinuous function of time $t$, prescribing the distance $d$ as a function of time, and requiring that the line OA remain fixed in B; see Fig. 1. Note that Eq. (2d) represents a linear interpolation in the stiffness value for the $n$th spring between its values at the beginning and end of extrusion of link $n+1$. This provides an accounting of the variable stiffness of the beam. The variable $n$ order-$n$ algorithm is now applied to this system during successive periods of time, during which the system has a constant $n$ degrees of freedom while one link is being extruded or retracted.

## Order-*n* Algorithm

Rosenthal's order-$n$ algorithm,[2] which is reviewed here with corrections to the published version, and modifications to accommodate variable $n$ and prescribed base motion, is based on Kane's method[15] and uses terminology such as generalized speeds, partial velocities, and partial angular velocities associated with Kane's equations. The algorithm is given here in the context of a system of rigid bodies connected in the form of a chain to a point that itself moves in a prescribed manner in a given reference frame. An arbitrary body is denoted by the index $k$ and the body preceding it by the index $i$, as in Fig. 2. The dynamical equations are formed in three passes: a forward pass for developing kinematical variables going from body $n$ to body 1, followed by a backward pass to form the dynamical equation for the $n$th body, and, finally, a forward pass for obtaining the remaining dynamical equations. It is assumed that each body $k$ has a basis vector associated with it.

#### Initialization Step

Specify starting value of $n$, numbering the bodies as shown in Fig. 1. Assign inertia properties, introducing intermediate bodies with zero mass and inertia when a hinge has more than one rotational degree of freedom. Compute the stiffness coefficients as per Eqs. (2). Initialize generalized coordinates $q_k$ and generalized speed $u_k = \dot{q}_k$ $(k = 1, \ldots, n)$ for all the hinge relative rotations. Prescribe the base motion and the extrusion rate (rate of change of the distance $d$ in Fig. 1) as functions of time.

#### Forward Pass

*Step 1.* Define the coordinate transformation matrix $C_{ik}$ between body $i$ and its outboard body $k$ for all $k$. The elements of $C_{ik}$ are

$$C_{ik}(1,m) = \bar{b}_i(1) \cdot \bar{b}_k(m) \qquad (k = n, \ldots, 1;\ 1,m = 1,2,3) \tag{3}$$

where $\bar{b}_i(m)$ is the $m$th component of the vector basis of the $i$th body.

*Step 2.* Form the angular velocity $\bar{\omega}^k$ of the $k$th body in the $k$ basis and define corresponding $3 \times 1$ matrices $\omega^k$ $(k = n, \ldots, 1)$ using the sequence

$$\bar{\omega}^n = \bar{\omega}^B + u_n \bar{\lambda}_n \tag{4a}$$

$$\bar{\omega}^k = \bar{\omega}^i + u_k \bar{\lambda}_k \qquad (k = n-1, \ldots, 1) \tag{4b}$$

where $\bar{\lambda}_k$ is the unit vector along the rotation axis for the $k$th hinge and $B$ is the reference body to which body $n$ is hinged and whose motion is prescribed. Note that the hinge-axis vectors are not restricted to be all parallel; this feature allows describing three-dimensional motion.

*Step 3.* Form the partial angular velocity of the $k$th body with respect to the $k$th generalized speed

$$\bar{\omega}_k^k = \bar{\lambda}_k \qquad (k = n, \ldots, 1) \tag{5}$$

in the $k$ basis, forming the $3 \times 1$ matrix $\omega_k^k$ $(k = n, \ldots, 1)$.

*Step 4.* Express the partial velocity of the mass center of the $k$th body with respect to the $k$th generalized speed in the $k$ basis,

$$\bar{v}_k^{k*} = -\bar{\omega}_k^k \times \bar{r}_2^k \qquad (k = n, \ldots, 1) \tag{6}$$

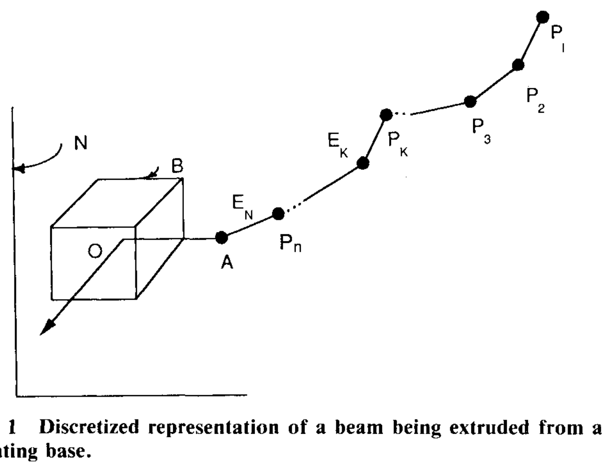


**Fig. 1 Discretized representation of a beam being extruded from a rotating base.**

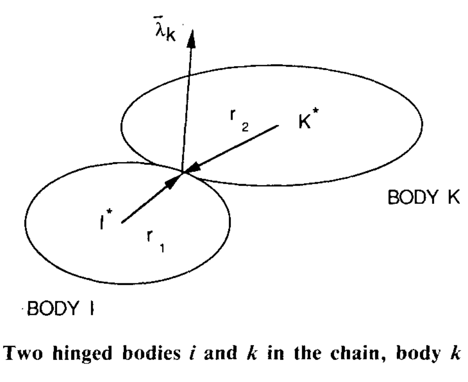


**Fig. 2 Two hinged bodies *i* and *k* in the chain, body *k* being outboard.**

Form corresponding $3 \times 1$ matrices $v_k^{k*}$ $(k = 1, \ldots, n)$. Note that $\bar{r}_2^k$ is the position vector going from the mass center of body $k$ to the $k$th joint, as in Fig. 2.

*Step 5.* Express the remainder term $\bar{\alpha}_t^k$ for the angular acceleration of the $k$th body defined as

$$\bar{\alpha}^k = \sum_{j=1}^{n} \bar{\omega}_j^k \dot{u}_j + \bar{\alpha}_t^k \qquad (k = n, \ldots, 1) \tag{7a}$$

$$\bar{\alpha}_t^n = \bar{\alpha}^B \tag{7b}$$

$$\bar{\alpha}_t^k = \bar{\alpha}_t^i + \bar{\omega}^k \times (u_k \lambda_k) \qquad (k = n-1, \ldots, 1) \tag{7c}$$

in the $k$ basis, forming the $3 \times 1$ matrix $\alpha_t^k$. Here, $\bar{\alpha}^B$ is the angular acceleration of the base to which the beam is attached.

*Step 6.* Express the remainder term $\bar{a}_t^{k*}$ of the acceleration of the mass center $k*$ of $k$

$$\bar{a}^{k*} = \sum_{j=1}^{n} \bar{v}_j^{k*} \dot{u}_j + \bar{a}_t^{k*} \qquad (k = n, \ldots, 1) \tag{8a}$$

$$\bar{a}_t^{n*} = \bar{a}^A - \bar{\omega}^n \times (\bar{\omega}^n \times \bar{r}_2^n) \tag{8b}$$

$$\bar{a}_t^{k*} = \bar{a}_t^{i*} + \bar{\alpha}^i \times \bar{r}_1^k + \bar{\omega}^i \times (\bar{\omega}^i \times \bar{r}_1^k) - \bar{\alpha}_t^k \times \bar{r}_2^k - \bar{\omega}^k \times (\bar{\omega}^k \times \bar{r}_2^k) \quad (k = n-1, \ldots, 1) \tag{8c}$$

in the $k$ basis forming the $3 \times 1$ matrix $a_t^{k*}$. Linear acceleration of the base of the beam is reflected in the term $\bar{a}^A$.

*Step 7.* For external force $F_k$ and external torque $T_k$, both expressed as $3 \times 1$ matrices in the $k$ basis, form the following $3 \times 1$ matrices:

$$F_t^{*k} = m_k a_t^{k*} - F^k \qquad (k = n, \ldots, 1) \tag{9a}$$

$$T_t^{*k} = I_k \alpha_t^k + \tilde{\omega}^k I_k \omega^k - T^k \qquad (k = n, \ldots, 1) \tag{9b}$$

where $\tilde{\omega}^k$ is the standard skew-symmetric matrix formed out of $\omega^k$.

*Step 8.* Form the $6 \times 6$ matrix $M_k$, the $6 \times 1$ matrix $X_k$, and the $6 \times 1$ matrix $Y_k$, $(k = n, \ldots, 1)$

$$M_k = \begin{bmatrix} m_k E & 0 \\ 0 & I_k \end{bmatrix} \tag{10a}$$

$$X_k = \begin{Bmatrix} F_t^{*k} \\ T_t^{*k} \end{Bmatrix} \tag{10b}$$

$$Y_k = \begin{Bmatrix} v_k^{k*} \\ \omega_k^k \end{Bmatrix} \tag{10c}$$

where $E$ is a $3 \times 3$ identity matrix and 0 is the $3 \times 3$ null matrix.

#### Backward Pass

*Step 1.* Set $k = 1$, $M = M_k$, $X = X_k$.

*Step 2.* Form and store the $6 \times 1$ matrix $Z_k$ and the scalars $m_{kk}$ and $f_k$ as follows:

$$Z_k = M Y_k \tag{11a}$$

$$m_{kk} = Y_k^t Z_k \tag{11b}$$

$$f_k = Y_k^t X + \tau_k \tag{11c}$$

where $\tau_k$ is the hinge torque applied by body $i$ on body $k$ at the $k$th hinge, and superscript $t$ on a matrix indicates its transpose. Form the $6 \times 6$ augmented mass matrix $M$ and the $6 \times 1$ augmented remainder inertia force matrix $X$,

$$M = M - [Z_k Z_k^t]/m_{kk} \tag{12a}$$

$$X = X - Z_k (f_k / m_{kk}) \tag{12b}$$

*Step 3.* Define the $6 \times 6$ shift transformation matrix $W$

$$W = \begin{bmatrix} C_{ik}^t & -\tilde{r}^{i*k*} C_{ik}^t \\ 0 & C_{ik}^t \end{bmatrix} \tag{13}$$

where $\tilde{r}^{i*k*}$ is the skew-symmetric matrix formed out of the components in the $k$-basis of the position vector going from the mass center $i*$ of body $i$ to the mass center of the $k$th body. Next, shift the inertia force and torque at the $k$th body, represented by the augmented mass and remainder inertia force matrices $M$ and $X$, to the $i$th body and add to the mass and inertia force matrices for the $i$th body

$$M = M_i + W^t M W \tag{14a}$$

$$X = X_i + W^t X \tag{14b}$$

*Step 4.* Increase $k$ by 1, and repeat steps 2 and 3 until $m_{nn}$ and $f_n$ have been computed.

#### Forward Pass

*Step 5.* Set $k = n - 1$ and $i = n$. Form the following:

$$\dot{u}_n = -f_n / m_{nn} \tag{15a}$$

$$\begin{Bmatrix} a_0^{i*} \\ \alpha_0^i \end{Bmatrix} = Y_n \dot{u}_n \tag{15b}$$

*Step 6.* Form the $6 \times 1$ matrices and the scalar derivative $\dot{u}_k$,

$$\begin{Bmatrix} \hat{a}_0^k \\ \hat{\alpha}_0^k \end{Bmatrix} = W \begin{Bmatrix} a_0^{i*} \\ \alpha_0^i \end{Bmatrix} \tag{16a}$$

$$\dot{u}_k = -\left( \{Z_k\}^t \begin{Bmatrix} \hat{a}_0^k \\ \hat{\alpha}_0^k \end{Bmatrix} + f_k \right) / m_{kk} \tag{16b}$$

$$\begin{Bmatrix} a_0^{k*} \\ \alpha_0^k \end{Bmatrix} = \begin{Bmatrix} \hat{a}_0^k \\ \hat{\alpha}_0^k \end{Bmatrix} + Y_k \dot{u}_k \tag{16c}$$

*Step 7.* Decrease the indices $k$ and $i$ by 1 and repeat step 6 until $\dot{u}_1$ is formed. It may finally be pointed out that the equations corresponding to Eqs. (12b) and (16b) given in Ref. 2 are incorrect.

#### Deployment Step

If one link has been extruded, replace $n$ by $n + 1$ and assume $q_{n+1} = \dot{u}_{n+1} = 0$. For retraction, replace $n$ by $n - 1$ when one link is retracted and update state as described later to maintain continuity in displacements and velocities. Reset the values of the beam stiffness coefficients based on Eqs. (2) for the current $n$. Go to step 1 of forward pass.

## Numerical Simulation

Before proceeding with the simulation for the extrusion problem, the order-$n$ algorithm, as presented here, was first tested for a constant $n$ with an independent check by a multibody code, DYNACON, developed at Lockheed Missiles & Space Company and based on the theory of Ref. 16. For a system of 20 hinge-connected bodies with two-degree-of-freedom hinges, released from an arbitrary initial configuration, the two codes produced exactly the same simulation results, with the order-$n$ simulation executing eight times faster than DYNACON. It is believed that programming with symbol manipulation and explicit coding would make the order-$n$ code run faster by greater factors.

The validity of modeling an extruding beam as a variable number of rigid rods connected by rotational springs is checked by comparing the results given by the present theory with a solution based on the conventional modal approach available in the recent literature. Reference 10 considered ex-

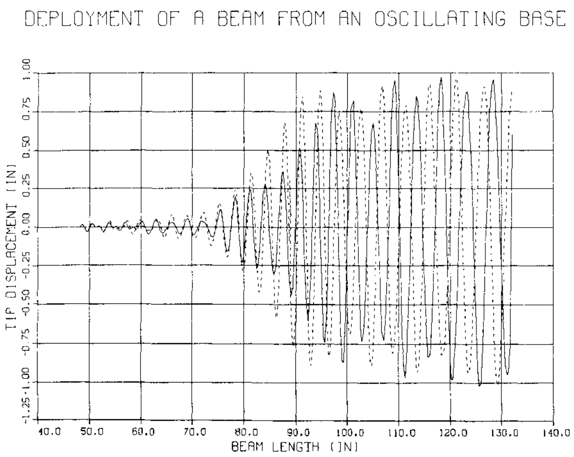


**Fig. 3 Extrusion of a beam from an oscillating base: present theory (solid line) vs theory of Ref. 10 (dashed line), which used time-varying shape functions, and did not include any dynamic stiffening effect.**

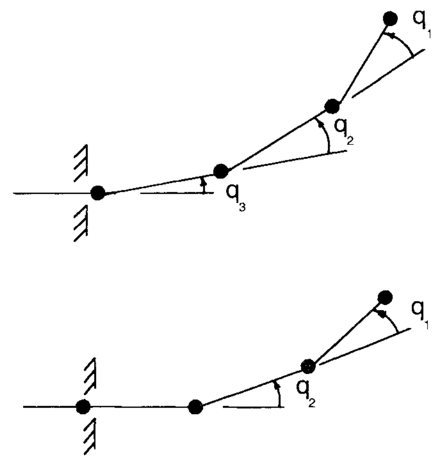


**Fig. 4 Schematic representation of jump discontinuity as one link goes in during retraction.**

trusion of a beam from a transversely oscillating base and modeled the beam as a Timoshenko beam with shear deformation and rotatory inertia; transverse deflection $v(x,t)$ and section rotation $\alpha(x,t)$ of the beam were assumed as

$$v(x,t) = \sum_{i=1}^{n} \left[\frac{x}{L(t)}\right]^i q_i(t) \tag{17a}$$

$$\alpha(x,t) = \sum_{i=1}^{n} \left[\frac{x}{L(t)}\right]^i s_i(t) \tag{17b}$$

where $L(t)$ is the time-varying length of the beam. The equivalent discrete spring coefficients needed for the model used in this paper are obtained by equating the continuum deflections for a beam under a tip force due to bending and shear with those given by the discrete model. This results in the modified stiffness coefficients (see Fig. 1),

$$k_1 = EI/L \tag{18a}$$

$$k_2 = nL/[L^2(3n-1)/(6EI) + 1/(\kappa AG)] \tag{18b}$$

$$k_i = k_1 \qquad i = 1, \ldots, n-1 \tag{18c}$$

$$k_n = k_2 + (k_1 - k_2)d/L \tag{18d}$$

where $L$ is the segment length, $A$ the cross-sectional area, $\kappa$ the shape factor, and $G$ the shear modulus. For a beam with a tip mass having a large rotary inertia, a base oscillation of amplitude 0.05 in. and frequency 1 Hz, and an axial deployment rate of 3 in./s, beam tip deflection is plotted in Fig. 3 as given by the present analysis and the analysis of Ref. 10 (using three modes) as the solid and dashed curves, respectively. It is seen that both curves indicate eventual resonance at 1 Hz, but the amplitude during transition to resonance and the phase subsequently are different in the two simulations. During transition, the solution given by Ref. 10 indicates an elastic system of less stiffness than that modeled by the method of this paper, and the consequent frequency difference propagates as a phase difference, subsequently. The reduced stiffness in the response in Ref. 10 can be attributed to premature linearization, inherent in the use of modes, which was not compensated for by the consideration of geometric stiffness due to base motion (see Ref. 17). By contrast, the present paper makes no linearization for its assumed physical model. Given the qualitative similarity of the two simulations and the reason for the differences, the discrete model used in this paper seems to be at least a reasonable and effective approximation.

In the examples on beam extrusion given later, base motion for the extruding body can be meaningfully prescribed. For the Shuttle/WISP/tether problems, prescribing deployment helps assess the disturbance for a control system design, and the required force can be applied as a feed-forward control. In the context of Fig. 1, this means that we consider at any time an $n$-body system anchored at point A to the rotating body $B$, whose motion is prescribed, with the acceleration of the anchor point A also prescribed. Thus, to start the kinematic forward pass, one has the following:

$$\bar{\omega}^B = \Omega(t)\bar{b}_3 \tag{19a}$$

$$\bar{\alpha}^B = \dot{\Omega}(t)\bar{b}_3 \tag{19b}$$

$$\bar{a}^A = (\ddot{d} - \Omega^2 d)\bar{b}_1 + (2\Omega\dot{d} + \dot{\Omega}d)\bar{b}_2 \tag{19c}$$

where $\bar{b}_1$, $\bar{b}_2$, and $\bar{b}_3$ are unit vectors fixed in $B$, and $d$ is the distance between O and A in Fig. 1. The variable $n$ order-$n$ algorithm is now used to simulate extrusions/retractions of the WISP antenna from a slowly rolling Shuttle. The antenna is taken to be a tube having a 0.0635-m diameter, 0.00254-m wall thickness, of mass density 0.3644 kg/m, and modulus of elasticity $1.96491 \times 10^{10}$N/m$^2$. Fully deployed, the antenna is 150 m long. It is assumed that the Shuttle rotates at a steady rate of 1 deg/s about an axis normal to the direction of extrusion/retraction. Extrusion from 5 to 150 m is simulated with the extrusion rate prescribed as

$$\dot{d} = v_{\max}\left[1 - \left(\frac{t}{t_{\max}}\right)^3\right] \tag{20}$$

and retraction from 150 to 5 m is simulated with the prescribed rate

$$\dot{d} = v_{\max}\left[1 - \left(\frac{t_{\max} - t}{t_{\max}}\right)^3\right] \tag{21}$$

with $v_{\max} = 0.26666$ m/s and $t_{\max} = 750$ s. Time taken to extrude or retract any one link, of length 5 m, of the discretized beam is calculated from Eq. (20) or (21), and the system degrees-of-freedom $n$ is held fixed for this duration. At the end of this duration, the number of links is increased by 1 in the case of extrusion and is reduced by 1 for retraction. For the case of retraction, this presents a situation of discontinuity in beam deflection between the $n$- and $(n-1)$-link systems, as indicated in Fig. 4. The initial values for the generalized coordinates and generalized speeds for a new set of links have to be computed on the basis of continuity of physical displacements and velocities between the new system and the old system. For retraction of a beam from a representative system of $n$ serial links (with single revolute joints between links) to a system of $n-1$ serial links, this requires that the following two equations for displacement and velocity be satisfied:

$$\sum_{j=i}^{n-1} L \sin \sum_{k=j}^{n-1} q_k^+ = \sum_{j=i}^{n} L \sin \sum_{k=j}^{n} q_k^- \qquad (i = 1, \ldots, n-1) \tag{22}$$

$$\sum_{j=i}^{n-1} L \sin \sum_{k=j}^{n-1} q_k^+ \sum_{l=j}^{n-1} \dot{q}_k^+ = \sum_{j=i}^{n} L \sin \sum_{k=j}^{n} q_k^- \sum_{l=j}^{n-1} \dot{q}_l^- \qquad (i = 1, \ldots, n-1) \tag{23}$$

Here, a variable with a superscript $^+$ indicates its unknown initial value for the system with $n-1$ links, wheras the same variable with a superscript $^-$ indicates its known value at the end of operation of the system with $n$ links. Note that Eq. (22) is nonlinear in the generalized coordinates, whereas Eq. (23) is linear in the generalized speeds. Equation (22), rewritten as $f_i = 0$ $(i = 1, \ldots, n-1)$, is solved by Newton's method, where the associated Jacobian matrix turns out to be triangular because the deflection at any revolute joint does not depend on the motion of the outboard links,

$$\frac{\partial f_i}{\partial q_j^+} = 0 \qquad j > i \tag{24a}$$

$$\frac{\partial f_i}{\partial q_i^+} = L \cos \sum_{k=i}^{n-1} q_k^+ \qquad (i = 1, \ldots, n-1) \tag{24b}$$

$$\frac{\partial f_i}{\partial q_j^+} = \frac{\partial f_i}{\partial q_{j-1}^+} + L \cos \sum_{k=j}^{n-1} q_k^+$$
$$(i = 1, \ldots, n-1;\ j = i+1, \ldots, n-1) \tag{24c}$$

The Newton updates are obtained by solving the linear equations

$$\left[\frac{\partial f}{\partial q}\right]_i (\{q\}_{i+1} - \{q\}_i) = -\{f\}_i \tag{25}$$

where the quantities within the brackets represent the Jacobian matrix; $\{q\}$ and $\{f\}$ denote, respectively, the generalized coordinates and functions in Eq. (22); and the subscripts denote iteration numbers. A criterion based on smallness of a norm of the right side of Eq. (25) is used for stopping the iterations. Finally, note that the coefficient matrix associated with the linear equations given by Eq. (23), which represents the partial velocities for the mass points $i$, $i = 1, \ldots, n-1$, is precisely the Jacobian matrix [in Eq. (25)], which represents the partial rate of change of position of these points with respect to the generalized coordinates. Note also that no initial value update of state is needed for extrusion since Eqs. (22) and (23) (with the superscripts $^+$ and $^-$ interchanged) are identically satisfied as the system grows from $n-1$ to $n$ elements, with the new element having zero transverse displacement and velocity.

Figures 5a and 5b show the transverse beam deflections during extrusion at the beam tip and at a point 50 m from the tip, respectively. The associated deployed length vs time is shown in Fig. 5c. From Figs 5a and 5c, it is seen that the beam tip deflection when the instantaneous length of the beam is about 130.5 m is 16.1 m. This is already a large deflection, beyond the range of validity of linear beam theory, so that any modal superposition approach would have been inapplicable. Note that extrusion from a rotating base makes the beam lag its original undeformed configuration in conformity with the nature of its Coriolis inertia loading; note also that the lumped mass at a distance of 50 m from the beam tip starts late in its transverse motion because this material point does not come out until a certain time that depends on the extrusion rate. Figures 6a and 6b show deflections at the beam tip and the 50 m point, respectively, during retraction. The corresponding retracted length vs time is given in Fig. 6c. From Figs. 6a and 6c, note that the beam tip defleciton when the instantaneous length of the beam is 133 m is about 23.0 m. This is quite a large deflection, even larger than that obtained with extrusion. Here, the beam leads the undeformed configuration due to the Coriolis inertia force associated with retraction; the oscillation of the point 50 m from the tip stops as it goes into the containing body, whereas as for the mass at the tip, the terminal oscillations in Figs. 6 show the transverse motion of the tip of a stubby beam that remains when retraction is ended.

The results of Figs. 6 demonstrate that deflections of a beam being retracted into a rotating body do not necessarily grow unbounded. This is in contrast to the well-known case of a tether being retrieved into an orbiting body where the tether has a tendency to wrap up because of which various stabilizing control laws have been proposed in the literature (see, e.g.,

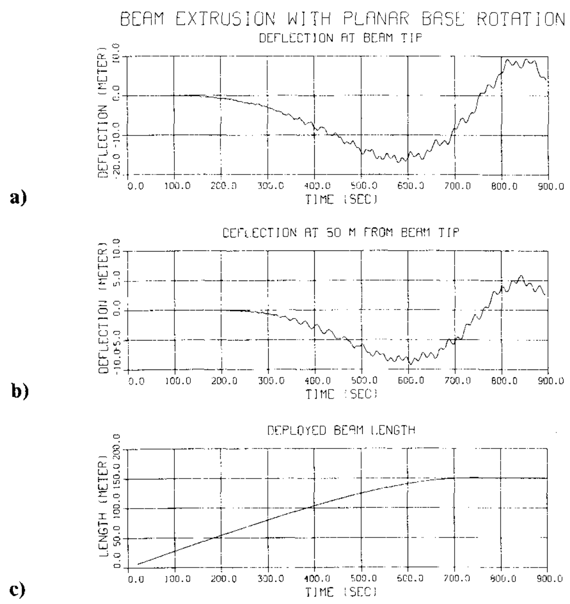


**Fig. 5 Transverse beam deflection during extrusion of a beam from a rotating base: a) at beam tip; b) at 50 m from beam tip; c) deployed beam length.**

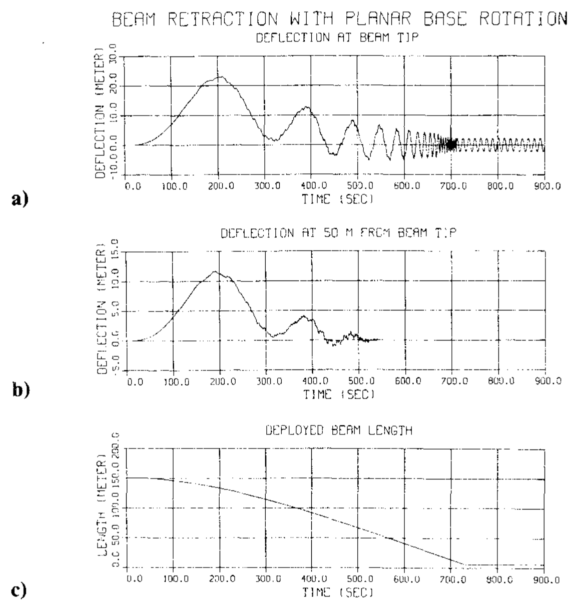


**Fig. 6 Transverse beam deflection during retraction of a beam into a rotating base: a) at beam tip; b) at 50 m from beam tip; c) deployed beam length.**

a)
b)
c)

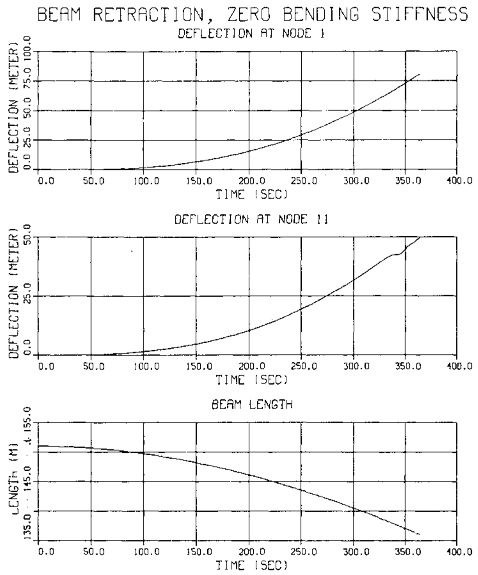


**Fig. 7 Transverse deflection and instantaneous length during retraction of a tether (beam of zero bending stiffness) into a rotating body: a) deflection at node 1; b) deflection at node 11; c) beam length.**

a)
b)
c)

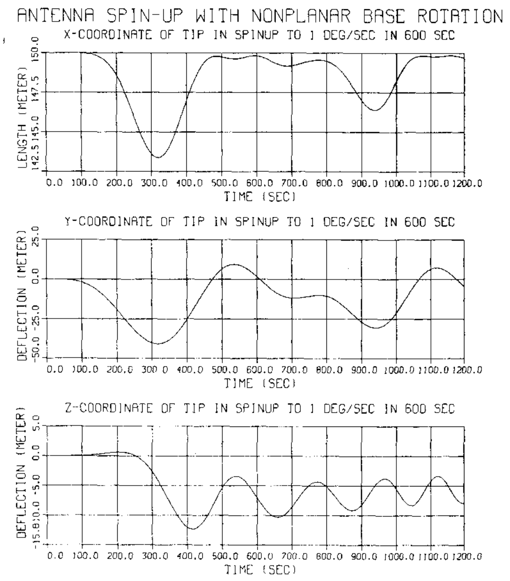


**Fig. 8 Three-dimensional deformation of a long, slender beam attached to a base undergoing spin-up to 1 deg/s in 600 s, with overall nonplanar rotation: a) *x* coordinate of tip; b) *y* coordinate of tip; c) *z* coordinate of tip.**

Ref. 18). Because of the fact that a tether can be thought of as a beam of zero bending stiffness, the method of this paper can be used for analysis of retraction of a tether into a rotating body. Figures 7 show three plots corresponding to the three plots of Figs. 6, respectively, for a zero stiffness beam retrieved at half the retraction rate used for generating Figs. 6. It is seen that the beam has very large deflection even at this reduced retraction rate with less than 15 m of retraction completed, and it tends to fly off much as a tether being retrieved into a rotating body is known to do. This indicates that it is the bending stiffness of a beam that prevents its deflection from growing unbounded during retraction into a rotating body.

Finally, to emphasize that the algorithm given in this paper can be used to describe three-dimensional motion, we consider the spin-up problem of a fixed length beam attached to a base undergoing nonplanar motion. Specifically, the base rotation is prescribed as

$$\bar{\omega}^B = 0.001\ \bar{b}_1 + \frac{0.0174533}{600}\left[t - \frac{300}{\pi}\sin\left(\frac{\pi t}{300}\right)\right]\bar{b}_3, \quad t \le 600$$
$$= 0.001\ \bar{b}_1 + 0.0174533\ \bar{b}_3, \qquad t > 600 \tag{26}$$

Such a base motion would, for example, describe the yaw spin-up of the Shuttle to 1 deg/s in 600 s as the Shuttle pitches around the orbit. Three-dimensional response of the beam was obtained by modeling two-degree-of-freedom rotational hinges at the joints of the rigid/elastic model. Figures 8 show the three-dimensional tip movement of the same 150-m-long slender antenna as used before, corresponding to the spin-up maneuver prescribed by Eqs. (26); Fig. 8a displays the $x$ coordinate of the beam tip, revealing axial foreshortening, and Figs. 8b and 8c show the extremely large transverse deflections of the beam during and subsequent to the spin-up. In practice, the stresses attendant with such large deflections may not be allowable, and this would preclude the use of such high spin-up rates.

## Conclusions

A computationally efficient simulation tool has been developed for studying large bending vibrations of a beam during its extrusion/retraction from/into a moving base. The order-$n$ algorithm provides considerable savings in computation time compared to coupled matrix formulations when $n$ is large; this allows a detailed study of the transient beam dynamics involving many elements to represent the beam. The formulation adapts Rosenthal's order-$n$ algorithm to a discrete model of the beam where the number $n$ of discrete elements is changed discontinuously according to a deployment scheme. It is shown by comparing to a conventional formulation using the time-varying modal approach that the representation of a beam by a series of rigid rods connected by rotational springs gives an effective approximation to the response when deflections are small. In situations where large overall motion with large elastic displacement is to be investigated, the modal superposition approach is inapplicable, whereas the approach used in this paper of working with direct physical coordinates is clearly valid. For the WISP boom problem studied in this paper, large bending deflections were shown to occur, with larger deflections occurring during retraction than in extrusion. For the tether problem, the simulations suggested that the lack of bending stiffness in a tether accentuates the bending deflections during retrieval. The simulation method developed can be used to analyze large overall three-dimensional motion including deployment of a beam with large elastic displacement.

## Acknowledgments

I am pleased to thank Dan Rosenthal for many helpful discussions in the course of my efforts to recreate the order-$n$ formulation. I am also thankful to Glenn Creamer of the Naval Research Lab for providing me with his results for the extrusion problem used for comparison in this paper.

## References

[1]Hollerbach, J. M., "A Recursive Lagrangian Formulation of Manipulator Dynamics and a Comparative Study of Dynamics Formulation Complexity," *IEEE Transactions on Systems, Man, and Cybernetics,* Vol. SMC-10, No. 11, 1980, pp. 730–736.

[2]Rosenthal, D. E., "An Order-N Formulation for Robotic Systems," *Journal of Astronautical Sciences,* Oct.–Dec. 1990, pp. 511–530.

[3]Rodriguez, G., "Spatially Recursive Filtering and Smoothing Methods for Multibody Dynamics," *Proceedings of the SDIO/NASA Workshop on Multibody Simulations,* edited by G. Man and R.

Laskin, Jet Propulsion Lab., Pasadena, CA, JPL Pub. D-5190, 1987, pp. 1094–1121.

[4]Bae, D. S., and Haug, E. J., "A Recursive Formulation for Constrained Mechanical System Dynamics: Part I, Open Loop Systems," *Mechanics of Structures and Machines,* Vol. 15, No. 3, 1987, pp. 359–382.

[5]Roberson, R. E., and Schwertassek, R., *Dynamics of Multibody Systems,* Springer-Verlag, Berlin, 1988.

[6]Keat, J. E., "Multibody System Order *n* Dynamics Formulation Based on Velocity Transform Method," *Journal of Guidance, Control, and Dynamics,* Vol. 13, No. 2, 1990, pp. 207–212.

[7]Tabarrok, B., Leech, C. M., and Kim, Y. I., "On the Dynamics of an Axially Moving Beam," *Journal of the Franklin Institute,* Vol. 297, No. 3, 1974, pp. 201–220.

[8]Cherchas, D. B., "Dynamics of Spin-Stabilized Satellites During Extension of Long Flexible Booms," *Journal of Spacecraft and Rockets,* Vol. 8, No. 7, 1971, pp. 802–804.

[9]Modi, V. J., and Ibrahim, A. M., "A General Formulation for Librational Dynamics of Spacecraft with Deploying Appendages," *Journal of Guidance, Control, and Dynamics,* Vol. 7, No. 5, 1984, pp. 563–569.

[10]Creamer, N. G., "On the Deployment of a Flexible Boom from an Oscillating Base," *Proceedings of the AIAA Dynamics Specialist Conference,* AIAA, Washington, DC, 1990, pp. 459–468.

[11]Lips, K. W., Graham, W. B., Vigneron, F. R., and Hunter, D. G., "Dynamics and Control Characteristics for the WISP 300m Dipole Antenna/Shuttle Configuration," *Advances in the Astronautical Sciences,* Vol. 58, Pt. 1, edited by H. Jacobs, AAS, San Diego, CA, 1985, pp. 349–370.

[12]Li, D., and Likins, P. W., "Dynamics of a Multibody System with Relative Translation on Curved, Flexible, Tracks," *Journal of Guidance, Control, and Dynamics,* Vol. 10, No. 3, 1987, pp. 299–306.

[13]Hwang, R. S., and Haug, E. J., "Translational Joints in Flexible Multibody Dynamics," *Proceedings of the 1988 ASME Design Automation Conference,* American Society of Mechanical Engineers, New York, 1988, pp. 435–445.

[14]Banerjee, A. K., and Kane, T. R., "Extrusion of a Beam from a Rotating Base," *Journal of Guidance, Control, and Dynamics,* Vol. 12, No. 2, 1989, pp. 140–146.

[15]Kane, T. R., and Levinson, D. A., *Dynamics,* McGraw-Hill, New York, 1985.

[16]Banerjee, A. K., and Lemak, M. E., "Multi-Flexible-Body Dynamics Capturing Motion-Induced Stiffness," *Journal of Applied Mechanics,* Vol. 58, No. 3, 1991, pp. 766–775.

[17]Banerjee, A. K., and Dickens, J. M., "Dynamics of an Arbitrary Flexible Body in Large Rotation and Translation," *Journal of Guidance, Control, and Dynamics,* Vol. 13, No. 2, 1990, pp. 221–227.

[18]Banerjee, A. K., and Kane, T. R., "Tethered Satellite Retrieval with Thruster Augmented Control," *Journal of Guidance, Control, and Dynamics,* Vol. 7, No. 1, 1984, pp. 45–50.